Upper Critical Solution Temperatures in Carbon Dioxide–Hydrocarbon Systems

Frederic Leder and Cyrus A. Irani[1]
Exxon Research and Engineering Co., P.O. Box 45, Linden, N.J. 07036

Critical solution temperatures of binary mixtures were measured, with particular interest being given to the situation in which one of the components is a gas near its critical temperature. The carbon dioxide–1,2,3,4,-tetrahydronaphthalene (tetralin) and the carbon dioxide–decahydronaphthalene (decalin) systems were studied. Phase diagrams analogous to the carbon dioxide–*n*-alkane systems ($>C_{13}$) were observed. Interactions between the strong carbon dioxide quadrapole and the aromatic structure of tetralin or naphthenic structure of decalin were not significant. A 25 wt % benzene + 75 wt % decalin–carbon dioxide system gave a continuous vapor-liquid critical locus between the pure component critical points, as did the binary systems carbon dioxide–benzene, carbon dioxide–cyclohexane, carbon dioxide–hexane, and carbon dioxide–1-hexene, in contrast to the unbounded critical loci of CO_2–decalin and tetralin. The experimental results tend to support the general conclusion that geometric considerations are dominant in determining the formation of a UCST line in the critical region.

An upper critical solution temperature (UCST) occurs when two immiscible phases become increasingly more miscible with increasing temperature. The UCST is the temperature corresponding to a maximum in the temperature-composition coexistence curve, at which the two phases merge into a homogeneous system, and is the maximum temperature at which the two phases can coexist.

The UCST phenomena are commonly found in mixtures of hydrocarbon and polar liquids, e.g., heptane–aniline. At lower temperatures the energy of interaction of the dipoles in the pure aniline is strong enough to dominate the free energy expression, i.e., the enthalpy change of mixing nonpolar molecules into a fluid held together by strong dipole-dipole interactions is large and positive. As the temperature is raised, the entropy term becomes more important; thus, miscibility increases with temperature. The balance of the kinetic energy by the energy of dipolar attraction of the pure component molecules leads to the upper critical solution temperature.

In systems of interest in this work, UCST phenomena occur above the critical point of the more volatile component and interact directly with the vapor-liquid critical envelope. Systems of this type were reported in 1903 by Kuenen (*4*) and later by Rowlinson and Freeman (*6, 7*) and Schneider (*8, 9*). An illustration of the UCST in the region of the vapor-liquid critical locus is shown in Figure 1, which is a sketch of the pressure-temperature projection of the critical region. By pressure-temperature projection of the critical locus, it is meant to imply that the data are points in pressure-temperature-composition space projected into the pressure-temperature plane. Thus, composition is a variable along such a projection, and this definition prevails throughout the work. Line A–C is the vapor pressure of the more volatile component from the triple point (C) to the critical point (A) of the pure component. Point B is the critical point of the less volatile component. The curve originating at B is the locus of critical points of the binary mixtures of the two components.

The critical locus appears to be quite normal until a minimum pressure is reached, at which point the locus rises to higher pressures at lower temperatures. At low temperatures and high pressure, i.e., below the critical temperature of the lighter component and pressure above the vapor pressure of the lighter component, two liquids exist. As the temperature is increased at constant pressure, e.g., along path E–F, the two phases become more miscible, until at point F (the UCST), the solution becomes homogeneous. Figure 1 may therefore be thought of as having "evolved" from Figure 2, in which the locus of UCST (L,L line in Figure 2) moves higher in temperature and intersects the vapor-liquid critical locus [see also (*9*)].

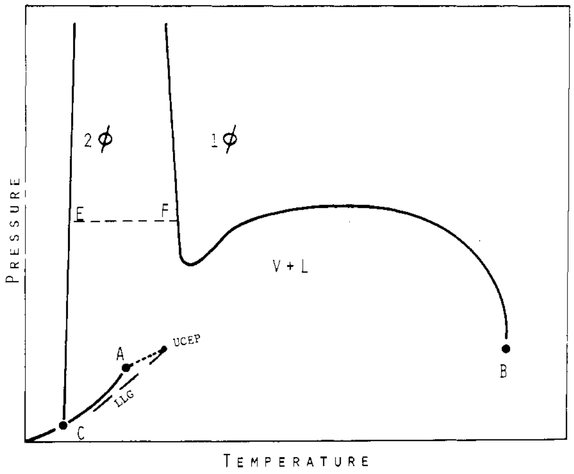

Figure 1. Pressure-temperature projection of discontinuous critical locus

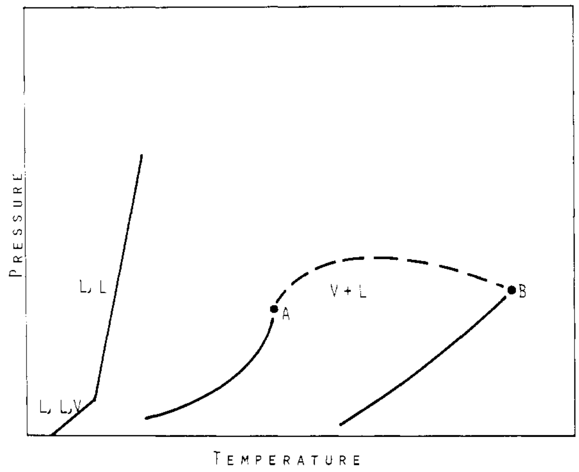

Figure 2. Pressure-temperature projection of continuous critical locus

---

[1] To whom correspondence should be addressed.

It is interesting to note that under such conditions, as illustrated in Figure 1, the gas becomes more soluble in the liquid as temperature is increased.

In consideration of the thermodynamics of UCST phenomena in the vapor-liquid critical region, it is now generally recognized (*7*) that entropy considerations can no longer be neglected on the assumption that the free energy term is dominated by the heat of mixing term. In this region both geometric and energetic factors are important in determining the shape of the critical locus.

Experimental

The sight glass unit used for this study is shown in Figure 3. The observations were made in a Jerguson Co. high-pressure sight glass fitted with a magnetic stirrer. The sight glass is made out of steel and equipped with two tempered borosilicate windows running along the central vertical axis of two opposing faces. The stirrer is an enclosed unit driven by a set of external magnets and is commercially available from Autoclave Engineers. Mixing action in the unit is achieved by two flat paddles attached to a ¼-in. diameter stainless-steel shaft which can be screwed into the main magnedrive shaft. A thermocouple well was drilled from the outside into one metal face of the sight glass to a distance ¼ in. from the working space. Accurate temperature control (±0.1°C) was obtained by immersing the entire sight glass assembly into a constant temperature bath. For the high-temperature studies a transparent high boiling hydrocarbon fluid (e.g., Exxon's Primol 355) was used. In the low-temperature studies, methanol was used as the circulating fluid. Pressure was read on a Heise gage to ±1 psi. The total cell volume was determined to be 30 cc.

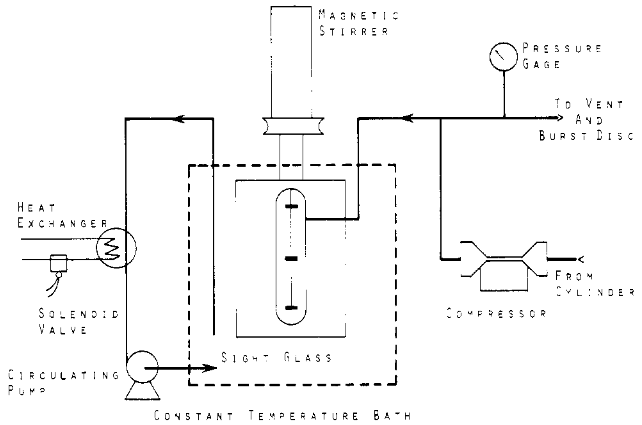

Figure 3. Schematic diagram of assembled apparatus

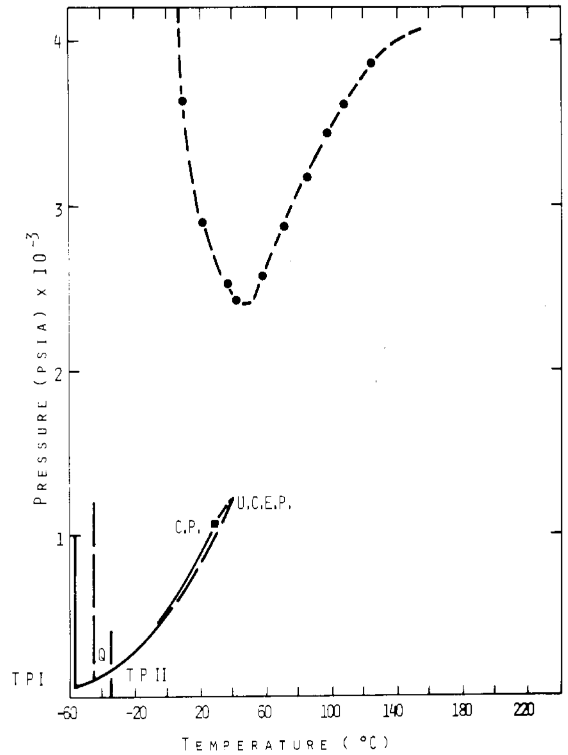

Figure 4. Pressure-temperature projection of critical locus of tetralin-CO_2 binaries: — = vapor-pressure curve (pure component); - - - = critical curve; — — — = three-phase LLG line; TPI = triple point CO_2; TPII = triple point tetralin; Q = quadruple point

An experimental procedure analogous to that for determining the critical density of a pure component was followed. The sight glass was first evacuated, and then a predetermined amount of the less volatile component was introduced through a syringe opening. Care was taken to ensure that the less volatile component originally charged was in excess of its critical concentration at the highest working temperature. The temperature was now raised to the highest point of interest, and the more volatile component introduced via a compressor. As the lighter compound is introduced, the meniscus rises and the entire cell fills with liquid. The cell is then partially vented, discarding some of the mixture present, and the procedure is repeated. At the critical point the meniscus is seen to disappear in the center of the window, and simultaneously critical opalescence is observed. The system is now cooled to a lower temperature, causing the heavier component to again be in excess over its critical concentration, and the search procedure is reinstituted. In the case of ternary systems, only single-phase mixtures were vented to minimize changing the benzene to decalin ratio. The critical points were reproducible to ±0.1°C and ±3 psia.

The chemicals used were as follows: CO_2: "bone-dry" grade 99.8% CO_2; ethane: cp grade 99.0% ethane 0.4% H_2; tetalin: practical grade 97.3%; decalin: practical grade 60.2% cis, 39.1% trans; benzene: spectro quality 99+%; cyclohexane: spectro quality 98.2%; *n*-hexane: chromatoquality 99+%; *n*-hexene: 99%.

Results and Discussion

In Figures 4 and 5, the results of the investigation of tetralin-CO_2 binaries are shown. The critical locus is dropping from 125° to what appears to be a point somewhat above the critical point of pure CO_2. At a temperature of 50°C, the locus ceases to drop in pressure but instead begins to rise to higher pressures as the temperature is lowered. Regions of complete miscibility lie above 2400 psia and within the "Vee" formed by the critical locus. The portion of the critical locus below 50° is the locus of UCST, representing the maximum temperature at which two phases can coexist at a given pressure. The diagram as a whole may be interpreted as the intrusion of the locus of UCST into the vapor-liquid critical region.

In the region of the vapor-pressure line of CO_2, a line of liquid-liquid-gas (LLG) immiscibility is found, as shown in Figure 5. There is an upper critical end point (UCEP) at 41°C, designating the upper limit of the LLG line. At the UCEP, the upper liquid phase and the vapor phase, both rich in CO_2, become identical. At the lower temperatures, the LLG line falls on the CO_2 vapor-pressure line, indicating very slight tetralin solubility in the CO_2-rich upper liquid, and negligible tetralin partial pressure in the gas phase.

To study the influence, if any, of the interaction of the strong quadrapole associated with CO_2 and the aromatic structure of the tetralin, a similar study was done with decalin (decahydronaphthalene) and CO_2. The decalin-CO_2 critical locus, shown in Figure 6, is remarkably similar to the tetralin locus. Both have LLG immiscibility and a UCEP at 41°C and 1210 psia. The minimum in the critical locus of the tetralin mixtures is about 5° higher in temperature and 200 psia higher in pressure. The UCST locus in decalin-CO_2 appears to rise more steeply than in tetralin, indicating less dependence on pressure. On the whole, the similarity of the two sets of data is striking, considering the fact that tetralin is partially aromatic and decalin is totally naphthenic. Apparently, the interaction of CO_2 with the aromatic structure of tetralin is only of secondary consequence, the dominant factor being the size disparity between the CO_2 and the C_{10} hydrocarbons.

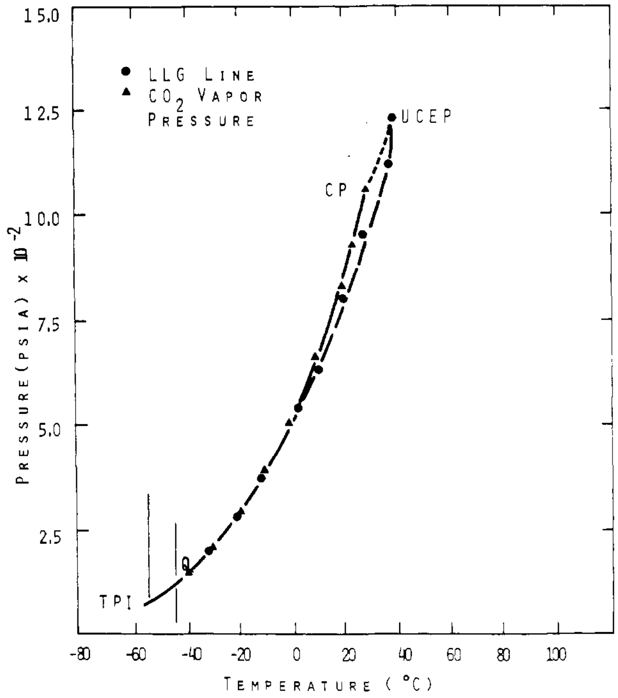

Figure 5. Pressure-temperature projection of critical locus of tetralin-CO_2 binaries: region of CO_2 critical point. TPI = triple point CO_2; Q = quadruple point

To further pursue the question of size disparity vs. aromatic and unsaturated bond interactions, the critical loci of CO_2 binary mixtures in benzene, cyclohexane, normal hexane, and normal hexene-1 were measured. These data are shown in Figure 7. The data for all these systems are also shown in Table I.

The critical loci of CO_2-benzene and CO_2-cyclohexane, as measured between 124° and 35°C, are indistinguishable, as are the loci of CO_2-*n*-hexane and CO_2-1-hexene. All four loci are continuous between the component critical points and show no UCST in the regions investigated. Disparities in size and shape appear to be the dominant factors in producing the UCST and in locating the critical locus. Aromatic rings and double-bond interactions appear to be of secondary consequence in these data.

In Figure 8, "pseudo" binary mixtures of decalin plus benzene in CO_2 are studied at fixed decalin-benzene ratios. In consideration of the benzene-CO_2 data as presented above, a slight inflection point appears to be located at about 40°C just below the UCEP. This inflection is more pronounced in the system, which is 25% benzene in decalin. In the 25% system, the locus is close to the CO_2-decalin locus at high pressures and temperatures but drops rapidly to the CO_2 critical point at low temperatures. The benzene appears to "bridge" the miscibility gap between CO_2 and decalin. No LLG was observed in this system.

At 10% benzene in decalin the critical locus is unbounded, exhibiting a UCST locus in the critical region. The small amount of benzene present is not sufficient to completely bridge the miscibility gap; however, the minimum in the criti-

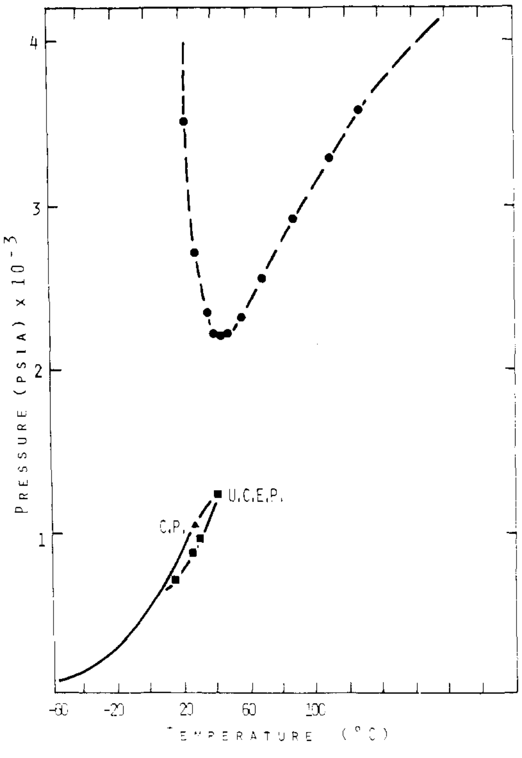

Figure 6. Pressure-temperature projection of critical locus of decalin-CO_2 binary

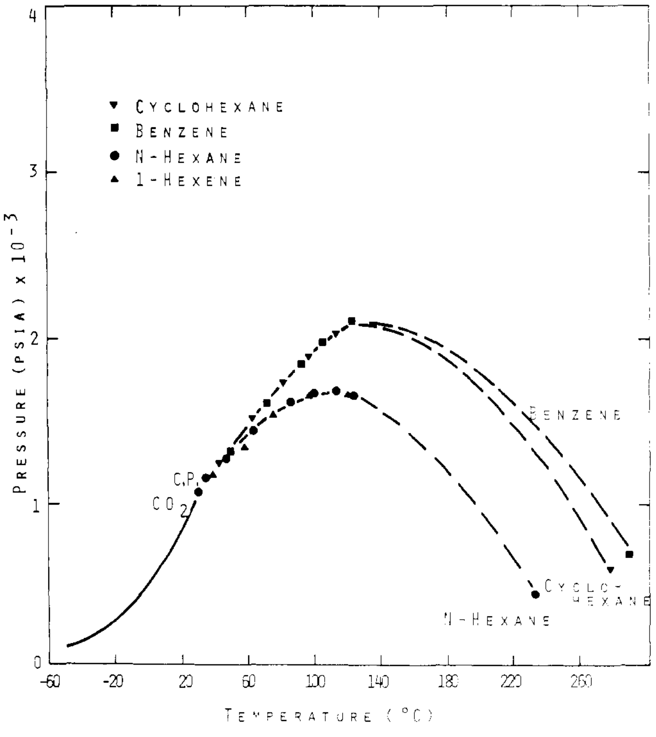

Figure 7. Critical loci of CO_2-hydrocarbon binary mixtures

cal locus is at 38°C and 1520 psia, considerably below the CO_2–decalin locus. The pressure required to bring about miscibility at the temperature of the minimum of the locus is reduced from 2200 psia to 1520, or about 60% of the pressure difference between the decalin–CO_2 minimum and the CO_2 critical pressure. Presumably, at a benzene concentration between 10 and 25%, the vapor-liquid critical locus would be continuous to the CO_2 critical point, and the UCST locus would appear below the CO_2 critical temperature. This set of data would completely demonstrate the evolutionary nature of the phase diagram formed by the intrusion of the UCST locus into the vapor-liquid critical region.

These data emphasize the importance of the entropy of mixing in causing a UCST to occur in the critical region, although obviously not to the exclusion of excess enthalpy, i.e., chemical interaction terms. Figure 9 shows the critical loci of

Table I. Pressure-Temperature Relations at Phase Boundaries for Various CO_2-Hydrocarbon Systems

CO_2 + tetralin

Temp, °C	Press, psia	
125.5	3868	L.L. critical
108.4	3620	L.L. critical
99.0	3433	L.L. critical
85.9	3177	L.L. critical
71.2	2873	L.L. critical
56.7	2570	L.L. critical
41.7	2393	L.L. critical
31.9	2426	L.L. critical
28.5	2520	L.L. critical
22.2	2904	L.L. critical
40.4	1229	UCEP
36.8	1142	LLG
27.5	954	LLG
20.5	805	LLG
10.3	636	LLG
3.8	538	LLG
0.0	494	LLG
−10.3	378	LLG
−20.6	285	LLG
−31.2	205	LLG
−44.2	124	Quad. pt. (SLLG)

CO_2 + benzene

Temp, °C	Press, psia
124.8	2100
106.8	1978
91.3	1841
72.0	1604
50.7	1312
38.1	1152
33.9	1102

CO_2 + 1-hexene

Temp, °C	Press, psia	
120.5	1662	Critical point
98.9	1638	Critical point
77.2	1534	Critical point
59.0	1378	Critical point
40.7	1186	Critical point
34.4	1135	Critical point
32.9	1103	Critical point

CO_2 + [decalin (90 wt %) + benzene (10 wt %)]

Temp, °C	Press, psia	
122.8	3300	L.L. critical
100.6	2973	L.L. critical
79.9	2563	L.L. critical
60.4	2038	L.L. critical
39.5	1528	L.L. critical
35.0	1534	L.L. critical
29.8	1609	L.L. critical
25.7	1830	L.L. critical
19.7	2511	L.L. critical
45.2	1308	UCEP
43.7	1277	LLG
40.5	1190	LLG
31.2	983	LLG
19.0	776	LLG
10.8	636	LLG
5.2	560	LLG

CO_2 + decalin

Temp, °C	Press, psia	
127.4	3492	L.L. critical
110.9	3282	L.L. critical
89.3	2926	L.L. critical
70.0	2547	L.L. critical
57.5	2316	L.L. critical
49.5	2218	L.L. critical
45.0	2197	L.L. critical
36.1	2340	L.L. critical
30.3	2712	L.L. critical
41.1	1240	UCEP
41.0	1237	LLG
38.0	1157	LLG
32.8	1047	LLG
25.1	889	LLG
14.9	704	LLG
4.9	557	LLG
0.5	500	LLG
−13.0	354	LLG
−25.8	241	LLG
−45.8	122	LLG
−55.3	83	LLG
−57.0	70	SLGG

CO_2 + *n*-hexane

Temp, °C	Press, psia
124.7	1662
115.9	1674
103.0	1659
86.5	1614
64.9	1449
47.9	1267

CO_2 + hexane

Temp, °C	Press, psia
114.4	2034
94.4	1876
87.6	1739
63.6	1491
44.2	1225

Ethane + decalin

Temp, °C	Press, psia	
121.8	1854	Critical point
100	1611	Critical point
79.1	1321	Critical point
49.6	892	Critical point

Ethane + benzene

Temp, °C	Press, psia	
121.8	1343	Critical point
100.3	1226	Critical point
77.8	1067	Critical point
49.3	837	Critical point

CO_2 + [decalin (75 wt %) + benzene (25 wt %)]

Temp, °C	Press, psia	
121.7	2965	Critical point
100.3	2646	Critical point
82.2	2288	Critical point
60.6	1715	Critical point
39.8	1199	Critical point

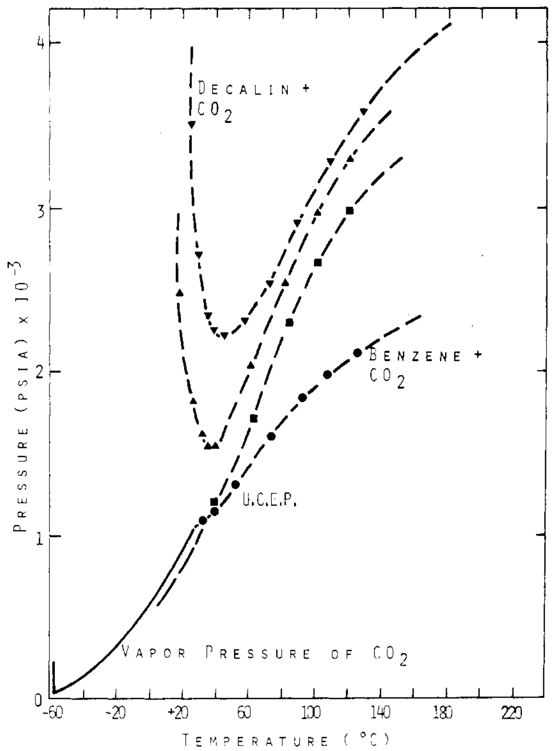

Figure 8. Pressure-temperature projections of critical loci of decalin–benzene–CO_2 mixtures: ■ = 25% benzene, 75% decalin + CO_2; ▲ = 10% benzene, 90% decalin + CO_2

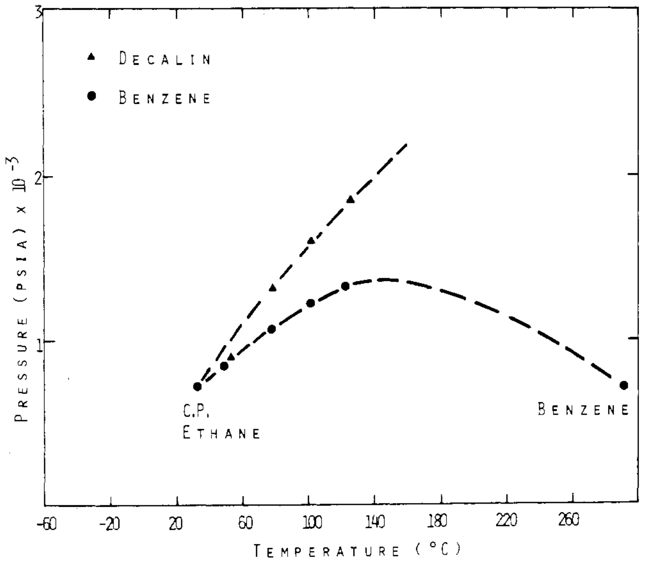

Figure 9. Pressure-temperature projections of critical loci of ethane–benzene and ethane–decalin binary mixtures

ethane–benzene and ethane–decalin mixtures. Ethane is a slightly larger molecule than CO_2, with very similar critical properties. In the case of ethane–decalin, the UCST has disappeared, and the critical locus is continuous between the two critical points. In the case of ethane–benzene, no UCST is observed, no inflection is observed in the locus of critical points, and the maximum in the critical locus is at 1360 psia, which is considerably below the 2100 psia observed with CO_2–benzene binaries.

Conclusions

The intrusion of a UCST locus into the vapor-liquid critical region of binary mixtures of CO_2 and C_{10} naphthenes has been observed. In CO_2–paraffin systems reported by Schneider (*9*), the intrusion into the critical locus does not occur until a carbon number of 16, indicating that in the critical region, a paraffin compound is more compatible with CO_2 than a naphthenic compound. The degree of hydrogenation is relatively unimportant in binaries of CO_2 and tetralin vs. decalin or CO_2 and cyclohexane vs. benzene, in which little or no difference is seen between the CO_2–hydrocarbon critical loci of the compounds being compared. The critical locus of CO_2–*n*-hexane is at lower pressure than CO_2–cyclohexane, indicating greater miscibility in the former system.

A UCST line forms in the critical region in CO_2 binaries of the 10 carbon naphthenes, tetralin and decalin, but the six carbon benzene does not show this behavior. This type of behavior is attributed to the size disparity between CO_2–decalin which is sufficient to influence the formation of a liquid-liquid type immiscibility near the CO_2 critical temperature. This size disparity effect can be minimized by the addition of benzene to the CO_2–decalin system, which causes the critical locus to revert to the continuous type. UCST behavior is not observed in the ethane–decalin system. The critical loci reported for the binary systems methane–*n*-heptane (*1*), methane–toluene (*2*), and methane–methylcyclohexane (*3*), when compared with the binary CO_2 systems reported here, tend to support the qualitative conclusion that the chemical nature and degree of hydrogenation are of minimal significance in such systems. Since size and shape considerations become of major importance in dealing with gas-liquid immiscibilities in the critical region, including those immiscibilities associated with upper critical solution temperatures, models based only on excess heats of mixing, e.g., regular solution theory, are not likely to be successful in predicting such phenomena.

Acknowledgment

The authors thank James A. McHenry for technical assistance in collecting the data.

Literature Cited

(1) Chang, H. L., Hurt, L. J., Kobayashi, R., *AIChE J.*, **12**, 1212 (1966).
(2) Chang, H. L., Kobayashi, R., *J. Chem. Eng. Data*, **12**, 517 (1967).
(3) Chang, H. L., Kobayashi, R., *ibid.*, p 523.
(4) Kuenen, J. P., *Phil. Mag. S.6*, **6** (36), 637 (Dec. 1903).
(5) Ricci, J. E., "The Phase Rule and Heterogeneous Equilibrium," Van Nostrand, New York, N.Y. 1951.
(6) Rowlinson, J. S., Freeman, P. I., *J. Pure Appl. Chem.*, **2**, 329–34 (1961).
(7) Rowlinson, J. S., "Liquids and Liquid Mixtures," Plenum Press, New York, N.Y., 1969.
(8) Schneider, G., *Ber. Bunsen Gas Phys. Chem.*, **70**, 497 (1966).
(9) Schneider, G., *CEP Symp. Ser.*, **64** (88), 9–15.

Received for review December 3, 1974. Accepted April 17, 1975.